

Article

A Novel Protection Strategy for Single Pole-to-Ground Fault in Multi-Terminal DC Distribution Network

Ruixiong Yang¹, Ke Fang², Jianfu Chen¹, Yong Chen¹, Min Liu^{2,*} and Qingxu Meng² 

¹ DC Power Distribution and Consumption Technology Research Center, Guangdong Power Grid Co., Ltd., Zhuhai 519099, China; gaga_xiong@163.com

² Energy and Electricity Research Center, Jinan University, Zhuhai 519070, China; tfangke@jnu.edu.cn

* Correspondence: liumin@jnu.edu.cn

Abstract: The single pole-to-ground (SPG) fault is one of critical failures which will have a serious impact on the stable operation of the multi-terminal DC distribution network based on the modular multilevel converter (MMC). It is very significant to analyze fault characteristics for detecting faults and protection design. This paper established the DC SPG fault model, which showed that in the presence of a reactor, the short-circuit current was reduced from 2.3 kA to 1 kA at 6 ms after the fault. Then, a novel SPG fault protection strategy was proposed, which detected the current derivative in connection transformer grounding branch. When the value increases past the threshold of current derivative, small resistance was switched on to increase fault current. Thus, the reliability of differential protection was enhanced. Compared with the traditional protection method, the proposed method does not need communication, and improved the speed of protection. Finally, the simulation model was established in PSCAD/EMTDC. The model included three converter stations: T1, T2 and T3. Among them, T1 outputs power, and T2 and T3 receive power. The results of RTDS showed that the DC circuit breaker operated within 3 ms, the three-port circuit breaker worked within 50 ms, which proves that the proposed strategy was effective. At this time, the system switched from the T1–T2–T3 three-terminal networking operation mode to the T1–T2 two-terminal hand-in-hand operation mode. Since the T3 terminal no longer received power, the transmission power of the T1 terminal decreased, and the received power of the T2 terminal remained unchanged.

Keywords: distribution network; single pole-to-ground (SPG) fault; multi-terminal DC; MMC; protection strategy; current derivative



Citation: Yang, R.; Fang, K.; Chen, J.; Chen, Y.; Liu, M.; Meng, Q. A Novel Protection Strategy for Single Pole-to-Ground Fault in Multi-Terminal DC Distribution Network. *Energies* **2023**, *16*, 2921. <https://doi.org/10.3390/en16062921>

Academic Editor: Georgios Christoforidis

Received: 17 January 2023

Revised: 10 March 2023

Accepted: 15 March 2023

Published: 22 March 2023



Copyright: © 2023 by the authors. Licensee MDPI, Basel, Switzerland. This article is an open access article distributed under the terms and conditions of the Creative Commons Attribution (CC BY) license (<https://creativecommons.org/licenses/by/4.0/>).

1. Introduction

With the maturity of flexible DC transmission technology and the continuous improvement of urban multi-load demand, multi-terminal DC (MTDC) distribution network became a research hotspot in the field of distribution network. The MTDC distribution network based on modular multilevel converter (MMC) has the advantages of higher reliability and economy, and it can adjust the power flow more flexibly, such as increasing power supply capacity, controlling active power and reactive power independently, reducing energy loss and operation cost. It became an important form of future energy [1,2]. However, the DC distribution network system has small damping and no natural zero-crossing point. Once a fault occurs on the DC side, the fault current will have a high peak value and a fast-rising speed, which will quickly spread to the entire power grid [3–5]. For a multi-terminal system, the superposition of short-circuit currents will bring further damage to the system, which puts forward higher requirements for the quickness of the protection scheme. Therefore, the protection of MTDC distribution network is one of the core technologies to be solved urgently.

In order to realize the operation safety of DC distribution, the protection technology is very important in researching DC distribution. The SPG fault is the most common fault,

which will lead the DC voltage unbalance. It will result in instability of DC distribution, which needs to be researched technically, such as fault detection and fault location.

On fault detection: fault detection methods can be divided into time-domain fault detection methods and frequency fault detection methods.

The time-domain fault detection method mainly judges whether a short-circuit fault occurs in the line by collecting and analyzing the voltage signal and the current signal of the DC line. On the one hand, referring to methods in traditional AC distribution networks, fault detection can be achieved by monitoring changes in current, voltage amplitude, or rate of change [6,7]. Although using the rate of change for fault detection can better distinguish the faulty line than directly using the current value, the fault detection using the rate of change is easily interfered by the sampling noise signal.

In addition to the fault detection based online sampling current and voltage, fault detection based on the difference of fault transient characteristics of line boundary elements is a unique fault detection method in the DC power grid [8].

In recent years, frequency-domain fault detection methods were proposed. Short-time Fourier transform and wavelet transform are two special forms of Fourier transform [9–12]. Although the frequency domain fault detection methods have high judgment accuracy and no threshold selection problem, the frequency domain fault detection methods need to convert the time domain signal into a frequency domain signal before data analysis. The frequency domain fault detection method requires a large amount of calculation, and the fault detection time interval is higher than that of the time domain fault detection method. To sum up, the time domain fault detection method is simple in calculation, it has extremely fast detection speed and the protection is also relatively sensitive. However, the time-domain fault detection method generally has the problem of threshold selection. Inappropriate threshold selection can easily lead to missed faults.

On the fault location, the methods can be divided into passive fault location methods and active fault location methods. The traveling wave method is a passive fault location method widely used in flexible HVDC transmission systems. However, the DC lines in the DC distribution network are much shorter than the lines in the DC transmission system. Thus, the transient traveling wave signal is weak. Therefore, the applicability of using the traveling wave method to fault location in the DC distribution network needs to be further demonstrated.

Compared with the passive fault location method, the active fault location method uses an additional circuit to inject electrical signals into the fault line and obtains the fault location by analyzing the change of the electrical signal in the fault line. In [13], the authors proposed a non-iterative fault location method using power detection units. The power detection unit injected detection power into the faulty line after the faulty line was cut off and inferred the location of the fault by analyzing the changes in the collected electrical signals. Additionally, this probe power can also be used for pilot testing prior to reclosing the main DCCB to avoid possible system problems when re-closing fails due to a permanent fault. Since the DCCB is close to the fault line, it has the location advantage required for injecting and detecting electrical signals in fault location. Therefore, the authors of [14] improved the DCCB to add a fault location function on the basis of the original fault interruption function. The improved DCCB can use its energy stored in advance to inject electrical signals into the fault line to realize the function of fault location. Compared with other active fault location methods, this method does not require an additional power supply, thereby reducing the cost and scale of fault location. In the ungrounded DC traction power system (asymmetric uni-polar wiring), the system can still operate normally when a single-phase ground fault occurs. If the fault is not detected and repaired in time, the fault type will change when the second ground fault occurs on the other pole. It is a short-circuit fault between poles, which seriously endangers the safe operation of the system. In order to solve this problem, the researchers in [15] proposed a method using a new type of power detection unit to detect and locate the ground fault. Compared with the traditional power

detection unit, the power detection unit in the literature can detect whether a short to ground fault occurred in the line in a timely manner.

Due to the short length of the DC line in the flexible DC distribution network, the fault circuit model can be equivalent to a lumped parameter circuit, and an active fault location method by injecting electrical signals and analyzing the RLC oscillation changes of the electrical signals was also proposed. Since the DC lines of the DC microgrid mostly use underground cables, the requirements for fault location accuracy are higher than those of the flexible DC transmission system using overhead lines. But for now, there is still no fault location method that considers both accuracy and economy in DC microgrids; so, the fault location method still needs further research and optimization.

Literature [4] proposed a handshake method to solve fault isolation and location in MTDC. Although DC circuit breaks are saved, lower action speed and worse action reliability of relays protection cannot satisfy the requirements. Literature [16] extracted the transient voltage oscillation characteristic-based Poly algorithm. By this method, although the fault distance can be calculated in several seconds, there is a dead zone. Literature [17] proposed a fault location method based on the active injection method, which can distinguish the fault zone by high frequency singles. However, this method requires much computation, and it is difficult to satisfy the requirements of fault isolation and location.

It follows that there are still many deficiencies in the existing protection schemes of flexible DC distribution network. In recent years, some scholars proposed a protection scheme for active control of the system after failure by utilizing the cooperation between the converter's own protection control function and protection strategy. In [18], the authors proposed a novel protection strategy to identify and locate SPG fault. In this method, a small resistor in parallel is used to increase the fault current. By detecting the current derivative in the connection transformer grounding branch, this method can quickly switch on a parallel resistor and eliminate the time of communication control, which greatly improves the speed of protection. Referring to the Zhuhai "Internet+" smart energy demonstration project [19], the system configuration and fault characteristics of MTDC were analyzed in detail. Finally, through the real-time digital simulator (RTDS), the feasibility of the proposed protection strategy was verified.

2. System Structure

2.1. MTDC Distribution Network Structure

In this paper, the MTDC distribution system was used, which is shown in Figure 1. T1–T3 are AC/DC converters based on MMC; T4 is the DC transformer; DCCBn ($n = 1, 2, \dots, 7$) represents the DC circuit breaker; ACCBn ($n = 1, 2, 3$) represents the AC circuit breaker; and f is the fault point. The system adopted the master–slave control mode, which has high control convenience [8], and T1 adopted the fixed DC voltage and reactive power control mode (VdcQ); T2–T3 adopted the constant power control mode (PQ). The system had a communication system to change control mode according to the situation.

2.2. Topology of MMC

The MMC included three parallel phase units: a, b, and c. Each phase unit consisted of upper and lower bridge arms. Each bridge arm contained n sub-modules and a reactor L_{arm} . In each sub-module, when SR was turned on and SF was turned off, the output voltage of the sub-module was the capacitor voltage; when SR was turned off, SF was turned on, the output voltage of the sub-module was 0; when both SR and SF were turned off, they were in blocking state.

The current control strategy of MMC generally adopted the D-Q decoupling control strategy in engineering. In the strategy, the modulation ratio M and the phase shift angle δ were controlled. Through modulation, the switching instructions of each sub-module were obtained with capacitor voltage equalization and circulating current suppression controller.

Through the turn-on and turn-off of the sub-module, the output voltage was obtained, which approached the modulation wave.

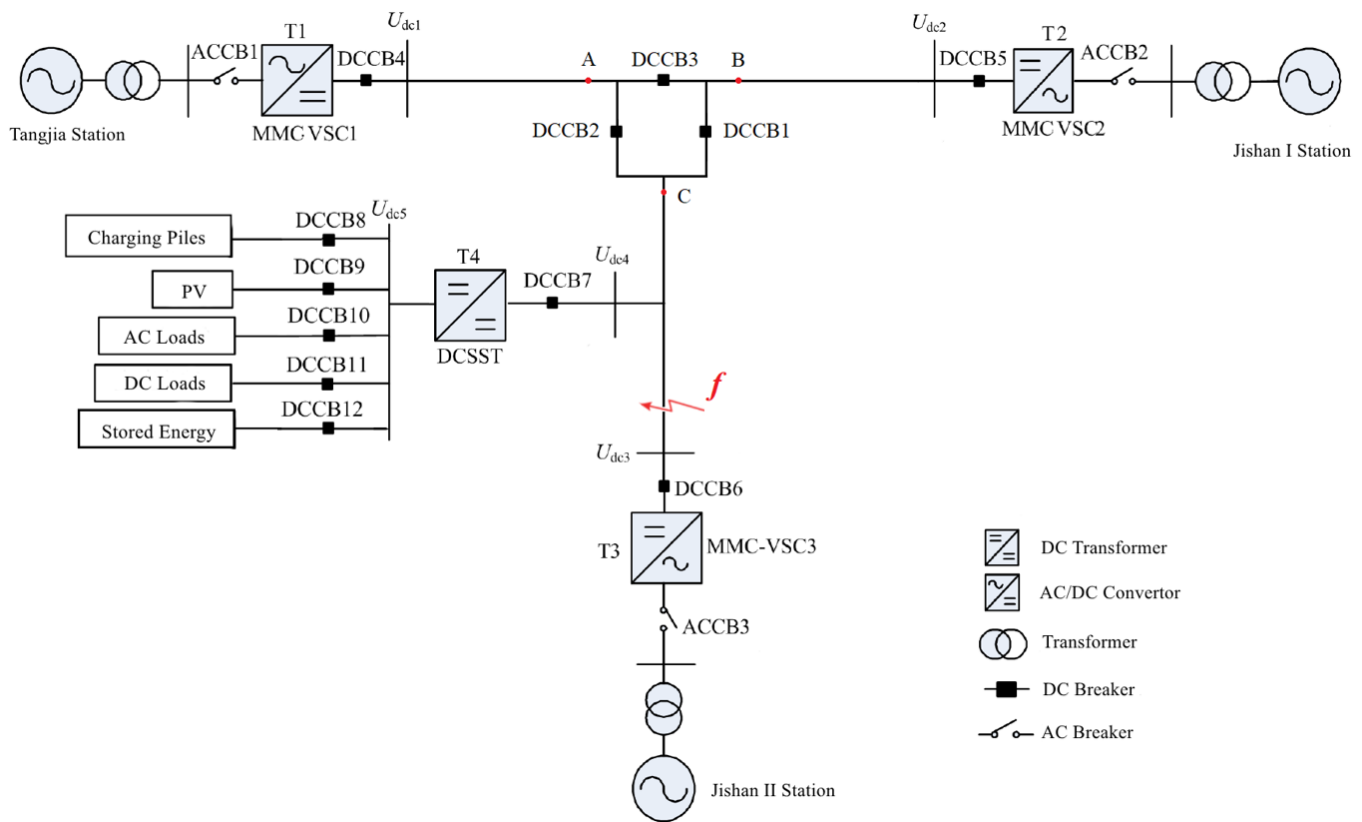


Figure 1. MTDC distribution network topology.

In a typical symmetrical bipolar MMC-HVDC system, in order to maintain the positive and negative symmetry of the DC bus voltage, it is necessary to set a grounding point on the DC side or converter transformer secondary side. Generally speaking, it can be divided into DC side grounding and AC side grounding. The grounding of the DC side is mainly grounded by clamping resistors in series between the DC positive and negative busbars, and the grounding of the AC side mainly includes the neutral point of the converter transformer being grounded through the resistor and the star-shaped reactance of the AC secondary side through the resistor, as seen in Figure 2. In this paper, the neutral point of the converter transformer being grounded through resistance in AC side was researched.

2.3. SPG Fault Model of MMC

Taking T3 as an example, the SPG fault model of MMC was established, as shown in Figure 1. After a single-pole ground fault occurs, due to the grounding of the AC side of the system, the capacitors of each faulty pole bridge arm will form a capacitive discharge path through the fault ground point and the AC side ground point. Taking the ground fault of the negative busbar as an example, the discharge path is indicated by red lines, which is shown in the Figure 2.

When a pole-to-pole fault occurs, the equivalent capacitance of the MMC can be deduced according to the law of energy conservation [7]. When a single pole ground fault occurs, the energy of the equivalent capacitance of the lower part of the three bridge arms should be equal to 1/2 DC bus voltage.

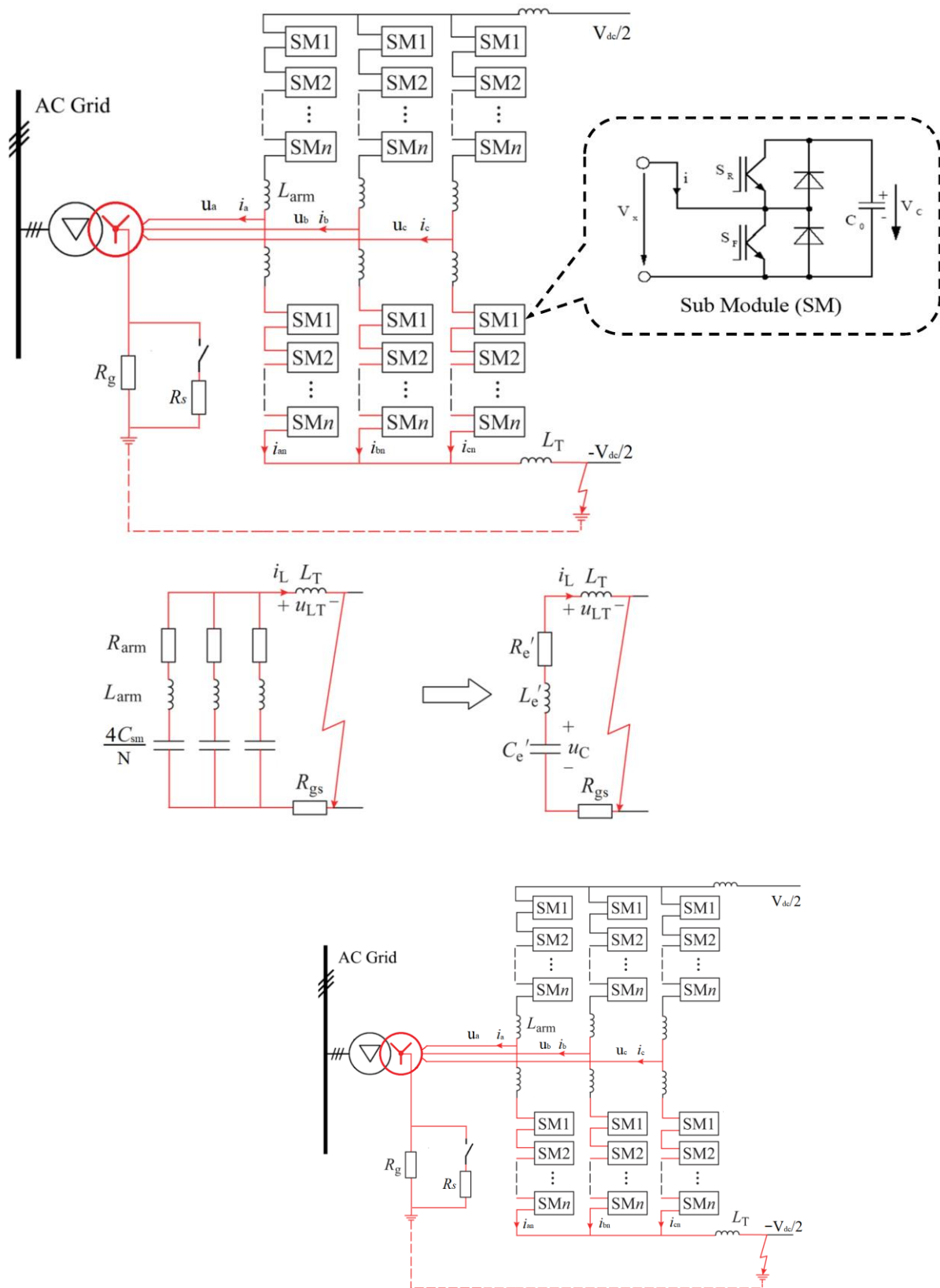


Figure 2. SPG fault model of MMC.

Assuming all SMs have the same voltage [7], the equivalent capacitor can be derived from

$$E_{MMC} = 3 * \frac{1}{2} C_{SM} \sum_{k=1}^n v_{C_k}^2 = \frac{1}{2} C'_e \left(\frac{1}{2} V_{dc} \right)^2 \tag{1}$$

$$3 * \frac{1}{2} C_{SM} n \left(\frac{V_{dc}}{n} \right)^2 = \frac{1}{2} C'_e \left(\frac{1}{2} V_{dc} \right)^2 \tag{2}$$

$$C'_e = \frac{12C_{SM}}{n} \tag{3}$$

It was seen that the equivalent capacitor of each bridge in pole-to-pole fault mode is $\frac{2C_{SM}}{n}$ [20], then equivalent capacitor of each bridge in SPG fault mode is $\frac{4C_{SM}}{n}$; finally, the equivalent capacitor of three bridges in parallel is $\frac{12C_{SM}}{n}$. Three resistance and inductance are also in parallel, and so, the equivalent resistance and inductance are

$$R'_e = \frac{1}{3} R_{arm}; L'_e = \frac{1}{3} L_{arm}$$

The equivalent parameters in the fault circuit are as follows:

$$\begin{cases} R_e = R'_e = \frac{1}{3} R_{arm} + R_{gs} \\ L_e = L'_e + L_T = \frac{1}{3} L_{arm} + L_T \\ C_e = C'_e = \frac{12C_{SM}}{n} \end{cases} \tag{4}$$

In the formula: R'_e is the equivalent resistance of MMC, L'_e is the equivalent inductance of MMC, C'_e is the equivalent capacitance of MMC; R_{arm} is the bridge arm equivalent resistance; L_{arm} is the bridge arm inductance; L_T is the DC reactor; R_{gs} which represents the parallel connection of R_g and R_s is the equivalent resistance of the neutral point of the connected transformer. The equivalent capacitor of each bridge and all bridges are $\frac{4C_{SM}}{n}$ and $\frac{12C_{SM}}{n}$, respectively.

$$i(t) = -\sum_{j=a,b,c} \frac{4}{n} \frac{d(v_{lowj})}{dt} \tag{5}$$

That is

$$I_0 = -12C_{SM} \frac{dv_c(t)}{dt} \tag{6}$$

The voltage is both ends of the capacitor.

$$\frac{d^2i}{dt^2} + \frac{R_e}{L_e} \frac{di}{dt} + \frac{1}{L_e R_e} i = 0 \tag{7}$$

Through Laplace transform, the discharge current of the converter station in Figure 2 is:

$$\begin{aligned} i(t) = & -\frac{i(0_-)}{\sqrt{1-\zeta^2}} e^{-\zeta\omega_n t} \sin(\omega_n \sqrt{1-\zeta^2} t - \varphi) \\ & + C u_c(0_-) \frac{\omega_n}{\sqrt{1-\zeta^2}} e^{-\zeta\omega_n t} \sin(\omega_n \sqrt{1-\zeta^2} t) \end{aligned} \tag{8}$$

$$i(8) \begin{cases} \omega_n = \frac{1}{\sqrt{LC}} \\ \zeta = \frac{R}{2} \sqrt{\frac{C}{L}} \\ \varphi_L = \arctan \sqrt{\frac{1}{\zeta^2} - 1} \end{cases} \tag{9}$$

where $i(t)$ is the fault current; $u_c(0_-)$ and $i(0_-)$ are the DC voltage and DC current of the converter station, respectively; t is the duration of the fault.

The number of sub-modules n of a single bridge arm of MMC is 25, the sub-module capacitance $C_{SM} = 15$ mF, the bridge arm inductance $L_{arm} = 7$ mH, the DC voltage

$u_{dc} = 10$ kV, bridge arm equivalent resistance $R_{arm} = 1 \Omega$, neutral grounding resistance $R_g = 2.5$ k Ω , $R_s = 625 \Omega$. Dyn11 wiring mode can be used to connect the transformer here to meet the DC side grounding requirements.

When $R_g = 0$, and R_s is cut off, the fault current is only suppressed by the DC reactor. According to the parameters of the converter station, the changing trend of the fault current with L_T is shown in Figure 3. When $L_T = 0$, $R_{gs} = 0$, the maximum fault current reaches 2.3 kA at 6 ms, which will reduce the reliability of the DCCB. The DC reactor can reduce the peak value and slope of the fault current. When $L_T = 0.0035$ H, the fault current is reduced to approximately 1 kA at 6 ms. In order to protect the safety of personnel and equipment, a large grounding resistance is usually set, and $R_g = 2.5$ k Ω can be set here.

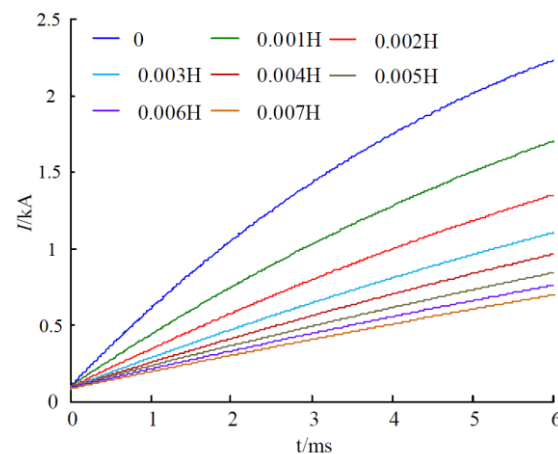


Figure 3. Relationship between fault current and inductance value.

3. Fault Criterion and Protection Scheme

3.1. Start Criterion of SPG Fault

At the beginning of the SPG short-circuit fault, due to the large resistance of the neutral point grounding, the short-circuit current is limited, the current flowing through the neutral point is less than 10 A. The DC pole voltage becomes unbalanced. DC voltage unbalance is used as main protection; the fault criterion is as follows:

$$|U_{dP}(t) + U_{dN}(t)| > U_{set} \quad (10)$$

In the formula, $U_{dP}(t)$ is the DC positive bus voltage; $U_{dN}(t)$ is the DC negative bus voltage; U_{set} is the constant value of the DC voltage unbalance protection setting, where $U_{set} = 0.2u_{dc}$. The protection is carried out under asymmetric fault, and it will not act under normal operation and symmetrical faults. Considering the reliability, 20% of rated DC voltage is selected as the value of action threshold.

3.2. Location Method of SPG Fault

Since the connection transformation was grounded by a high resistance, the fault current was small under SPG fault. Under this condition, differential protection cannot satisfy the requirements of protection action and reliability. This means that detection and location of fault cannot be obtained by differential protection. This paper proposed a fast fault location method. Current derivative at grounding resistance of connection transformer was monitored. When SPG fault occurs, the value of current derivative will rise remarkably. Therefore, when the value of current derivative increases to above the threshold, the small resistance will be switched on, which will lead to raise fault current value to satisfy the requirement of differential protection. The method above determines the fault location and classification in concert with voltage unbalance protection. Current derivative reduces the detection of fault current, and it does not require communication.

3.2.1. Differential Protection Action Criterion

Different from the DC voltage unbalance protection, the differential protection can determine the fault location in principle. In order to improve sensitivity, this paper applied the differential protection based on the zero-mode current.

Assuming that the fault occurs in DC side of Jishan II station, both ends are M, N , respectively, i_{M0}, i_{N0} are zero-mode current.

$$\begin{cases} i_{M0} = \frac{\sqrt{2}}{2}(i_{Mp} + i_{Mn}) \\ i_{N0} = \frac{\sqrt{2}}{2}(i_{Np} + i_{Nn}) \end{cases} \quad (11)$$

where i_{Mp}, i_{Mn} are positive current and negative current at M side, respectively, i_{Np}, i_{Nn} are positive current and negative current at N side, respectively.

The differential protection criterion is as follows,

$$|i_{M0} + i_{N0}| > \max(I_{C,set,L}, k_{set,L}I_{res,L}) \quad (12)$$

where the threshold value of differential current $I_{C,set,L} = 0.02I_{DC.Base}$; breaking current $I_{res,L} = \max(i_{M0}, i_{N0})$; breaking coefficient $k_{set,L} = 0.02$.

3.2.2. The Threshold Value of Current Derivative

The fault current derivative can be obtained from the (7).

$$dI = \frac{di}{dt} = \frac{V_{dc}}{2L_e} e^{-\frac{R_e}{L_e}t} \quad (13)$$

So, the value threshold of current derivative can be presented:

$$dI_{set} = k_{set} \max\left(\left|\frac{V_{dc}}{2L_e} e^{-\frac{R_e}{L_e}t}\right|\right) \quad (14)$$

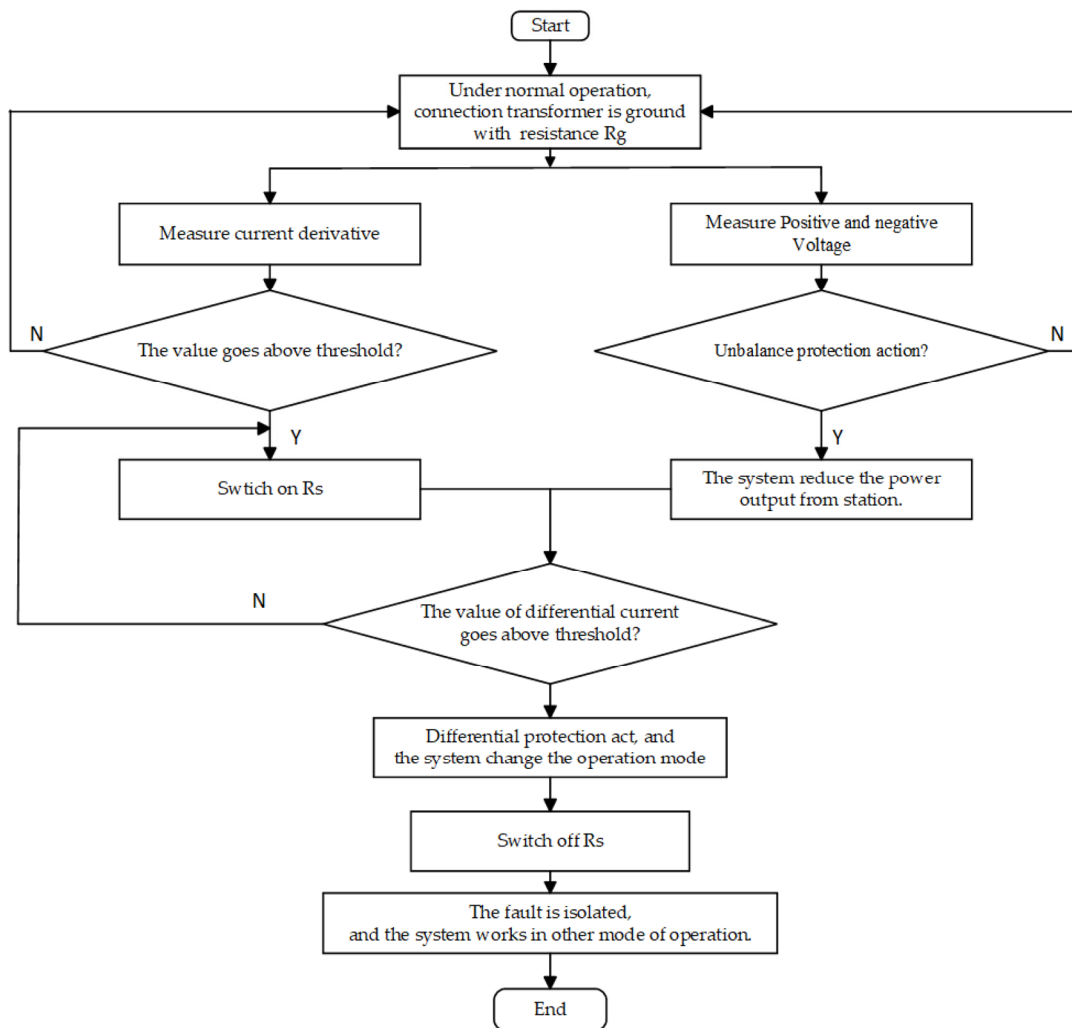
where k_{set} is coefficient of current derivative.

3.3. Protection Strategy

The protection scheme is as follows:

- (1) The DC power distribution control and protection system detects the change of the DC voltage according to the Formula (4). Whether the voltage unbalance occurs will be judged in the system. Meanwhile, the current derivative is detected according the Formula (13);
- (2) If voltage unbalance is detected, the system reduces the power output. If the value of current derivative exceeds the threshold, the neutral point grounding small resistance R_s is switched on to increase the fault current rapidly;
- (3) If Formulas (10) and (14) are satisfied at the same time, it is judged that a SPG fault has occurred. After that the small resistance is switched off, and then, the fault isolation and system operation state transition procedures are entered.

The flow chart of SPG fault protection strategy Scheme 1 for DC lines is as follows:



Scheme 1. The flow chart of SPG fault protection strategy.

4. Experiment and Simulation

The MTDC distribution network studied here had five operating modes, including three-terminal networking, two-terminal hand in hand, two-terminal isolated, single-terminal supply, STATCOM, etc. The direction and magnitude of the DC transmission power can be adjusted according to the flow of the AC power grid, realizing the unified coordinated control of the active and reactive power of the ± 10 kV DC power grid and the 10 kV AC power grid.

According to the topology in Figure 1, the model of multi-terminal DC distribution network was built based on PSCAD/EMTDC, in which the MMC converter was composed of six bridge arm components and bridge arm reactance, as shown in Figure 4. These were the three-port DC circuit breaker, which was composed of three fast mechanical switches, DCCB1, DCCB2, and DCCB3, two bidirectional power electronic switches, U1 and U2, and two energy absorption branches, R1 and R2. Among them, arbitrarily DC lines were, respectively, connected to two adjacent DC lines through the two fast mechanical switches in the hybrid DC circuit breaker to carry normal current, arbitrarily DC lines were connected to the bidirectional power electronic switch in the DC circuit breaker for bidirectional carrying and cutting off the fault current, each bidirectional power electronic switch was connected in parallel with the energy absorbing branch to absorb the energy stored in the fault line and limited the overvoltage when the bidirectional power electronic switch operated. The main circuit model is shown in Figure 4, where T1 was connected

to port A, T2 was connected to port B, and T3 was connected to port C. In Table 1, the parameters of T1–T3 are shown. The results of RTDS are shown in Figures 5–8.

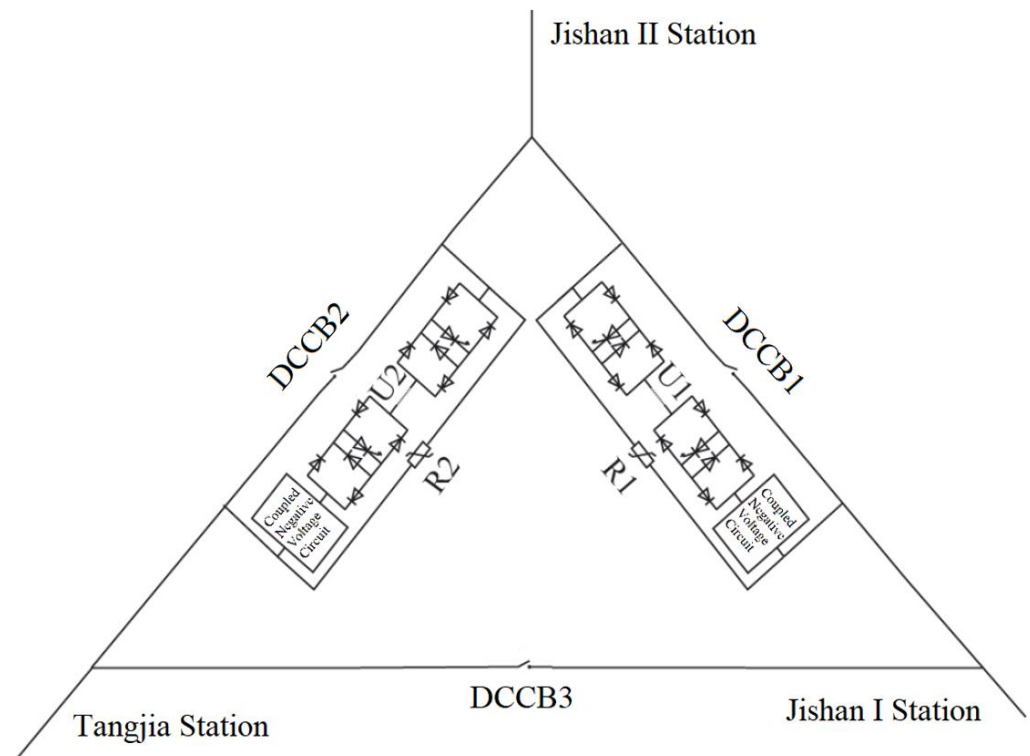


Figure 4. Three-port circuit breaker model.

Table 1. Parameters of the three-terminal VSC converter.

VSC No.	T1	T2	T3
Rated Power (MW)	20	10	10
AC grid voltage (kV)	10	10	10
DC bus voltage (kV)	± 10	± 10	± 10
Submodule topology	half bridge	half bridge	half bridge
Number of single-arm submodules	25	25	25
Submodule Capacitance (mF)	30	15	15
Bridge arm reactance (mH)	3.5	7	7
Transformer capacity (MVA)	24	12	12
Short circuit impedance ratio (%)	10	10	10
Winding Type	Dyn11	Dyn11	Dyn11
DC reactor (mH)	8	8	8

When the system operated normally, the three-terminal AC side supplied power to the DC distribution network by the ring network and realized flexible power transfer. At this time, the system worked in the three-terminal networking mode. T1 worked with fixed DC voltage control (VDCQ) mode, and T2 and T3 used power control (PQ) mode. The initial states of T1, T2, T3 are shown in Table 2.

Table 2. Initial states of T1–T3.

VSC No.	T1	T2	T3
AC system capacity	2 MVA	1 MVA	1 MVA
AC voltage level	10 kV	10 kV	10 kV
control mode	VdcQ	PQ	PQ

Before the fault occurred, $i_{T3P} = 40 \text{ A}$, $i_{T3N} = -40 \text{ A}$, $i_{T3NP} = 0 \text{ A}$. When $t = 6.61 \text{ s}$, a ground fault occurred at the DC negative pole of T3. The system detected an imbalance between positive voltage and negative voltage. At this time, the minimum value of i_{T3P} reached -30 A , the minimum value of i_{T3N} reached -200 A , and the peak value of the neutral point current was 5.2 A , which was far less than the short-circuit current of 1.5 kA in the related research [10]. It can be considered that the negative ground fault had a greater impact on the negative current than on the positive current. After 3 ms , the system turned on the small resistance $R_s = 650 \Omega$, and confirmed that it was a SPG fault. When $t = 6.613 \text{ s}$, the DC positive and negative poles tripped the DC circuit breaker, $i_{T3P} = 0 \text{ A}$, $i_{T3N} = 0 \text{ A}$. The three-port DC circuit breakers DCCB2 and DCCB3 connected to T3 were tripped at the moment of 6.662 s , and T3 was isolated. Figure 5 shows the DC positive current, DC negative current, and neutral point current of T3.

When $t = 6.61 \text{ s}$, ACCB3 and DCCB6 were tripped to break the AC line and isolate T3. When $t = 6.662 \text{ s}$, DCCB2 and DCCB3 were tripped to isolate T3, T4. Figure 6 shows the action sequence of the AC circuit breaker, DC circuit breaker, and three-port circuit breaker.

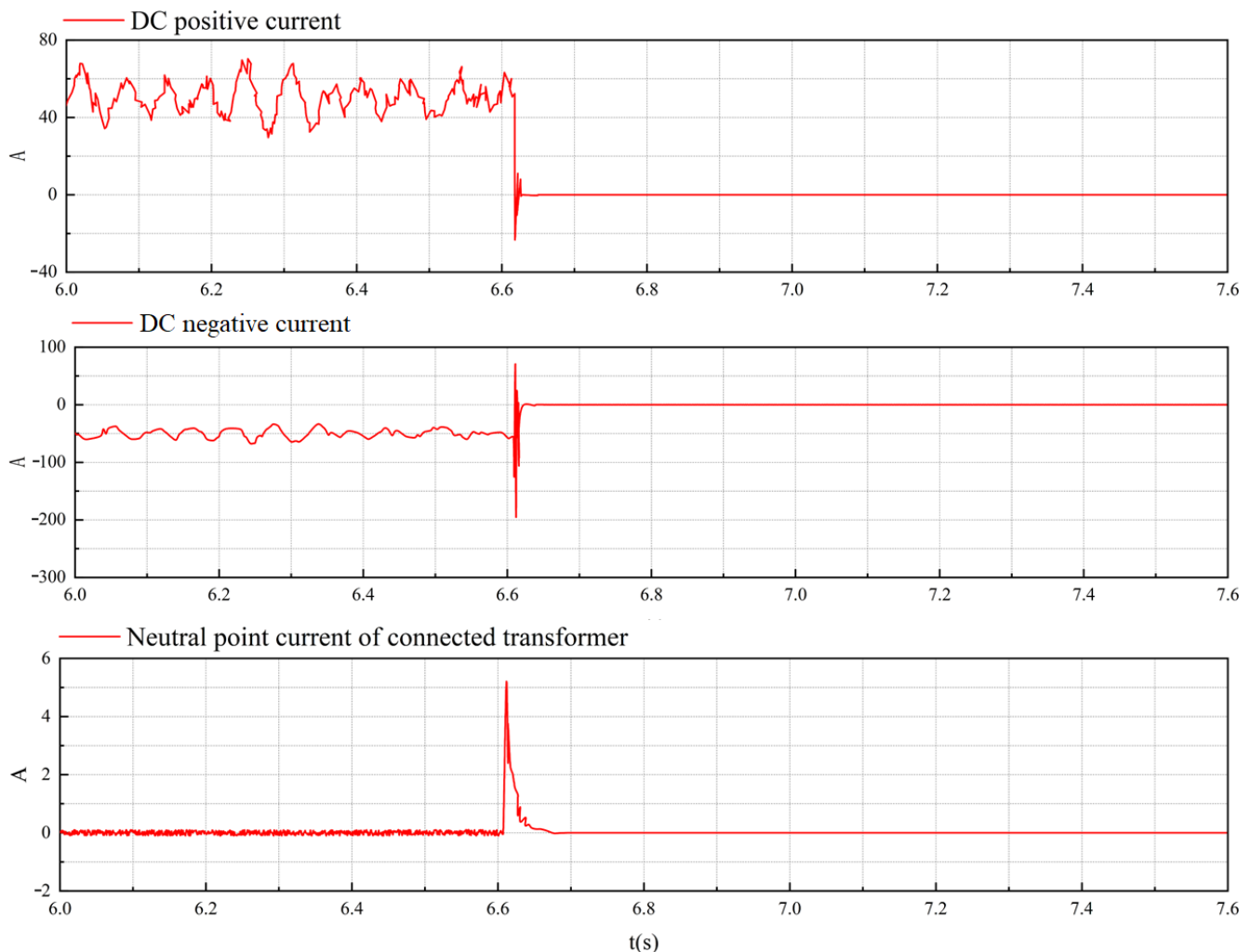


Figure 5. DC side current and neutral point current of T3.

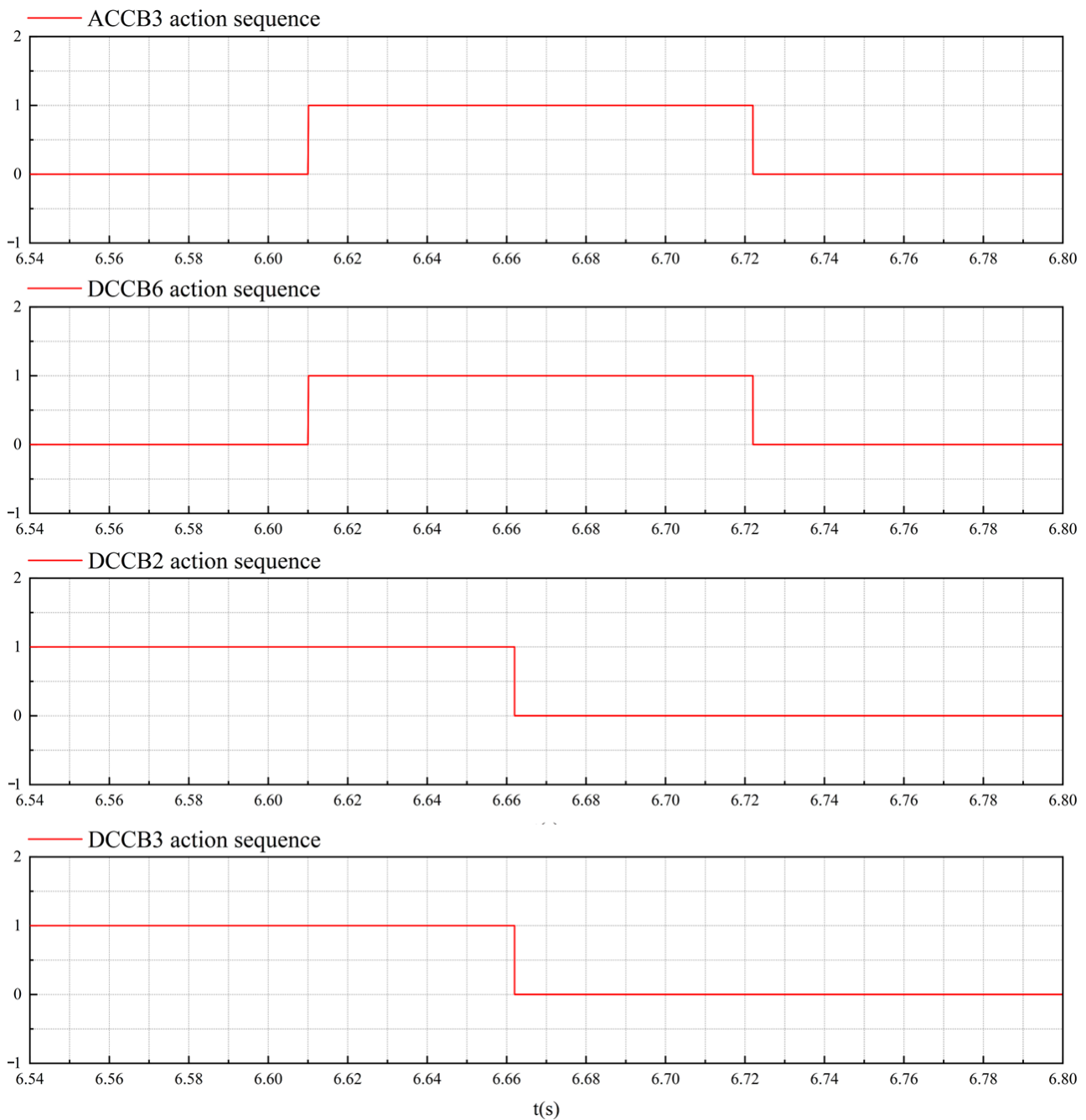


Figure 6. ACCB3, DCCB6, DCCB2, and DCCB3 action sequences.

Before the fault occurred, $u_{T1P} = 10$ kV, $u_{T1N} = -10$ kV, $i_{T1P} = -100$ A, $i_{T1N} = 100$ A. Affected by the SPG fault of T3, the DC positive and negative voltages increased by 10 kV at the same time due to fault disturbance. However, the power output from T1 became small. The DCCB2 and DCCB3 tripped at $t = 6.662$ s, u_{T1P} and u_{T1N} returned to normal levels at $t = 6.8$ s, and the current became small, $i_{T1P} = -50$ A, $i_{T1N} = 50$ A. Each parameter's waveform of T1 is shown in Figure 7.

T2 was also affected by T3. The DC positive and negative voltages increased by 10 kV at the same time. After the three-port circuit breaker trips, the T2 voltage returned to the normal level at $t = 6.8$ s. The positive and negative currents had an evident jitter at 6.615 s, but the steady-state amplitude changed little. Each parameter's waveform of T2 is shown in Figure 8.

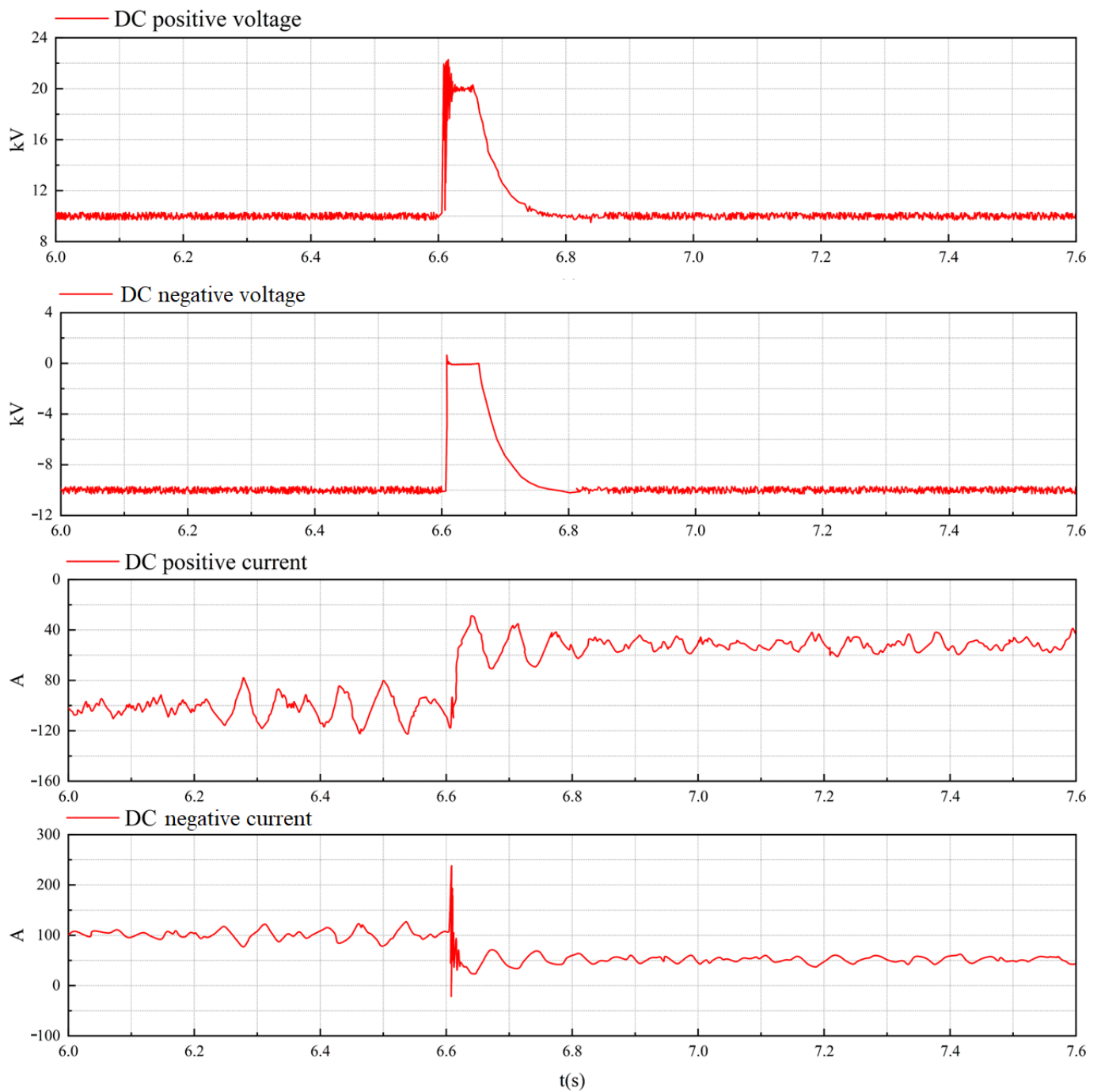


Figure 7. Waveforms of T1.

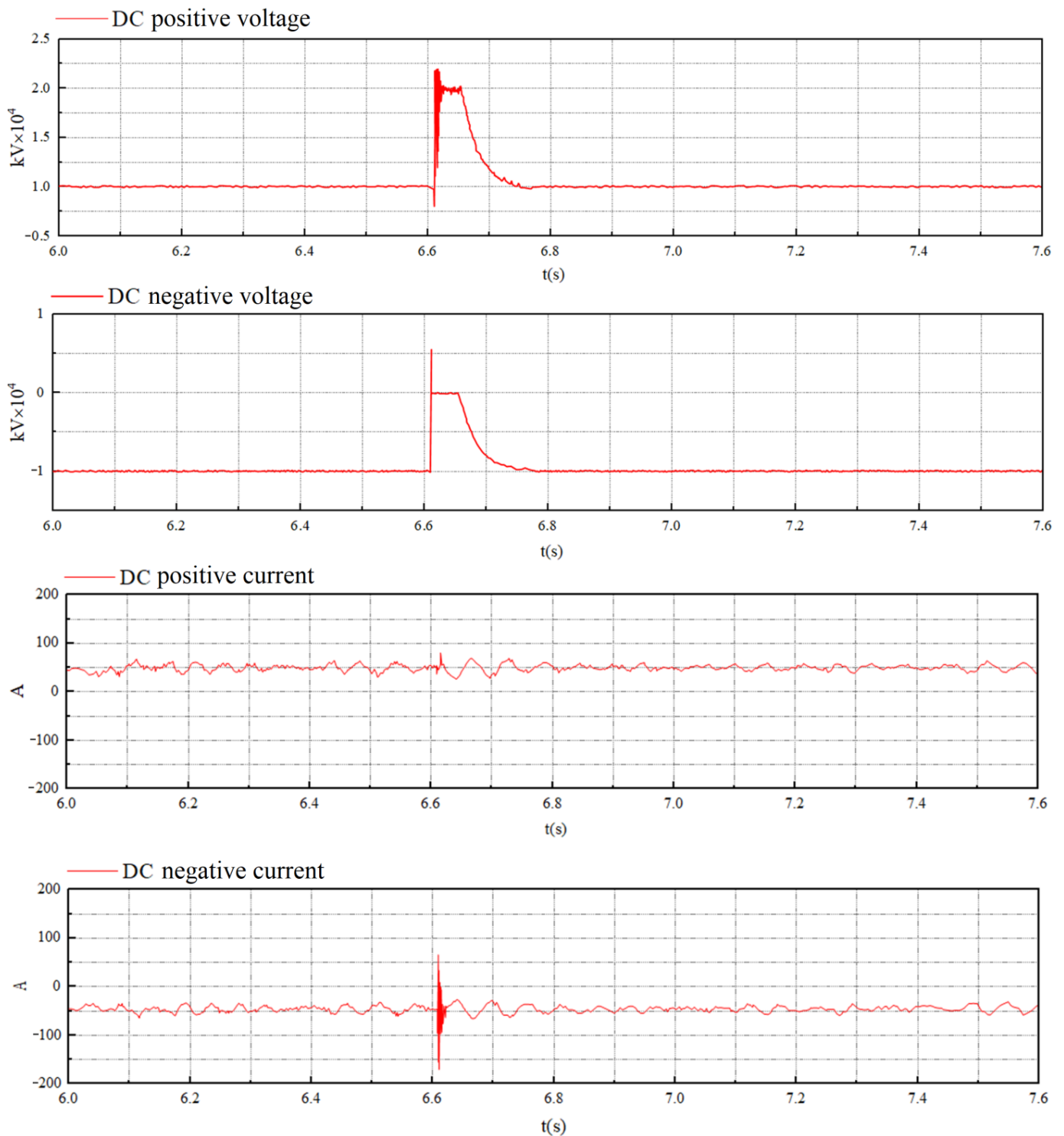


Figure 8. Waveforms of T2.

5. Conclusions

1. The comprehensive use of DC reactor and neutral point grounding resistance of connection transformer is an effective means to reduce the cost of fault removal and improve the economy of the system;
2. The criterion proposed can quickly detect the DC SPG fault. Voltage unbalance protection is used as main protection. In order to locate the fault, the method of

- switching the small resistance by detecting current derivative is proposed. The value of fault current rises rapidly so that reliability of differential protection can be satisfied;
3. The fault of T2 had a momentous effect on the power supply quality of other converter stations during SPG fault. The results proved that T2 can be isolated in time by three port DCCB. The operating mode of system was switched from the three-terminal network to two-terminal hand-in-hand. In future research, it will be necessary to study the influence of other faults on the MTDC distribution network. In addition, the voltage control mode of the converter station is also an important research field.

Author Contributions: Conceptualization, R.Y. and M.L.; Methodology, K.F.; Validation, M.L.; Investigation, Q.M.; Resources, Y.C.; Writing—original draft, K.F.; Supervision, J.C. All authors have read and agreed to the published version of the manuscript.

Funding: This work was financially supported by the Science and Technology Project of China Southern Power Grid, project number: 030600KK52190185 (GDKJXM20198191).

Data Availability Statement: Data is unavailable due to privacy.

Conflicts of Interest: The authors declare no conflict of interest.

References

1. Abedin, T.; Lipu, M.S.H.; Hannan, M.A.; Ker, P.J.; Rahman, S.A.; Yaw, C.T.; Tiong, S.K.; Muttaqi, K.M. Dynamic modeling of hvdc for power system stability assessment: A review, issues, and recommendations. *Energies* **2021**, *14*, 4829. [[CrossRef](#)]
2. Stan, A.; Costinaş, S.; Ion, G. Overview and Assessment of HVDC Current Applications and Future Trends. *Energies* **2022**, *15*, 1193. [[CrossRef](#)]
3. Farhadi, M.; Mohammed, O.A. Protection of multi-terminal and distributed DC systems: Design challenges and techniques. *Electr. Power Syst. Res.* **2017**, *143*, 715–727. [[CrossRef](#)]
4. Tang, L.; Ooi, B.T. Locating and isolating DC faults in multi-terminal DC systems. *IEEE Trans. Power Deliv.* **2007**, *22*, 1877–1884. [[CrossRef](#)]
5. Le Blond, S.; Bertho, R., Jr.; Coury, D.V.; Vieira, J.C.M. Design of protection schemes for multi-terminal HVDC systems. *Renew. Sustain. Energy Rev.* **2016**, *56*, 965–974. [[CrossRef](#)]
6. Monadi, M.; Koch-Ciobotaru, C.; Luna, A.; Candela, J.I.; Rodriguez, P. A protection strategy for fault detection and location for multi-terminal MVDC distribution systems with renewable energy systems. In Proceedings of the 2014 International Conference on Renewable Energy Research and Application (ICRERA), Milwaukee, WI, USA, 19–22 October 2014; IEEE: Piscataway, NJ, USA, 2014; pp. 496–501.
7. Meghwani, A.; Srivastava, S.C.; Chakrabarti, S. A new protection scheme for DC microgrid using line current derivative. In Proceedings of the 2015 IEEE Power & Energy Society General Meeting, Denver, CO, USA, 26–30 July 2015; IEEE: Piscataway, NJ, USA, 2015; pp. 1–5.
8. Dai, Z.; Liu, X.; He, Y.; Huang, M. Single-terminal quantity based line protection for ring flexible DC distribution grids. *IEEE Trans. Power Deliv.* **2019**, *35*, 310–323. [[CrossRef](#)]
9. Yeap, Y.M.; Geddada, N.; Satpathi, K.; Ukil, A. Time-and frequency-domain fault detection in a VSC-interfaced experimental DC test system. *IEEE Trans. Ind. Inform.* **2018**, *14*, 4353–4364. [[CrossRef](#)]
10. Li, B.; He, J.; Li, Y.; Ou, Y. Single-ended protection scheme based on boundary characteristic for the multi-terminal VSC-based DC distribution system. *Proc. CSEE* **2016**, *36*, 5741–5749.
11. He, J.; Li, B.; Li, Y.; Qiu, H.; Wang, C.; Dai, D. A fast directional pilot protection scheme for the MMC-based MTDC grid. *Proc. CSEE* **2017**, *37*, 6878–6887.
12. Xie, Z.; Zou, G.; Du, X.; Gao, H.L. Fast DC lines protection for symmetrical bipolar based MTDC grid. In Proceedings of the CSEE 2020, Virtual, 18–20 October 2020; Volume 40, pp. 1906–1915.
13. Kheirollahi, R.; Dehghanpour, E. Developing a new fault location topology for DC microgrid systems. In Proceedings of the 2016 7th Power Electronics and Drive Systems Technologies Conference (PEDSTC), Tehran, Iran, 16–18 February 2016; IEEE: Piscataway, NJ, USA, 2016; pp. 297–301.
14. Liu, W.; Liu, F.; Zha, X.; Huang, M.; Chen, C.; Zhuang, Y. An improved SSCB combining fault interruption and fault location functions for DC line short-circuit fault protection. *IEEE Trans. Power Deliv.* **2018**, *34*, 858–868. [[CrossRef](#)]
15. Park, J.D. Ground fault detection and location for ungrounded DC traction power systems. *IEEE Trans. Veh. Technol.* **2015**, *64*, 5667–5676. [[CrossRef](#)]
16. Jia, K.; Li, M.; Bi, T.; Yang, Q. A voltage resonance-based single-ended online fault location algorithm for DC distribution networks. *Sci. China Technol. Sci.* **2016**, *59*, 721–729. [[CrossRef](#)]
17. Jia, K.; Christopher, E.; Thomas, D.; Sumner, M.; Bi, T. Advanced DC zonal marine power system protection. *IET Gener. Transm. Distrib.* **2014**, *8*, 301–309. [[CrossRef](#)]

18. Xue, S.M.; Liu, C.J.; Li, Z.; Lu, J.C. Ranging Protection of Ring DC Microgrid System Based on Control and Protection Cooperation. *High Volt. Eng.* **2019**, *45*, 3059–3067.
19. Qu, L.; Yu, Z.; Song, Q.; Yuan, Z.; Zhao, B.; Yao, D.; Chen, J.; Liu, Y.; Zeng, R. Planning and analysis of the demonstration project of the MVDC distribution network in Zhuhai. *Front. Energy* **2019**, *13*, 120–130. [[CrossRef](#)]
20. Xu, Z.; Xiao, H.; Xiao, L.; Zhang, Z. DC fault analysis and clearance solutions of MMC-HVDC systems. *Energies* **2018**, *11*, 941. [[CrossRef](#)]

Disclaimer/Publisher’s Note: The statements, opinions and data contained in all publications are solely those of the individual author(s) and contributor(s) and not of MDPI and/or the editor(s). MDPI and/or the editor(s) disclaim responsibility for any injury to people or property resulting from any ideas, methods, instructions or products referred to in the content.